Bessel–Gauss photon beams with fractional order vortex propagation in weak non-Kolmogorov turbulence

Jie Gao,[1] Yu Zhu,[1] Donglin Wang,[1] Yixin Zhang,[1,2,*] Zhengda Hu,[1,2] and Mingjian Cheng[3]

[1]*School of Science, Jiangnan University, Wuxi 214122, China*
[2]*Jiangsu Provincial Research Center of Light Industrial Optoelectronic Engineering and Technology, Wuxi 214122, China*
[3]*School of Physics and Optoelectronic Engineering, Xidian University, Xi'an 710071, China*
**Corresponding author: zyx@jiangnan.edu.cn*

Received October 21, 2015; revised December 8, 2015; accepted December 21, 2015;
posted December 23, 2015 (Doc. ID 252458); published February 22, 2016

We model the effects of weak fluctuations on the probability densities and normalized powers of vortex models for the Bessel–Gauss photon beam with fractional topological charge in the paraxial non-Kolmogorov turbulence channel. We find that probability density of signal vortex models is a function of deviation from the center of the photon beam, and the farther away from the beam center it is, the smaller the probability density is. For fractional topological charge, the average probability densities of signal/crosstalk vortex modes oscillate along the beam radius except the half-integer order. As the beam waist of the photon source grows, the average probability density of signal and crosstalk vortex modes grow together. Moreover, the peak of the average probability density of crosstalk vortex modes shifts outward from the beam center as the beam waist gets larger. The results also show that the smaller index of non-Kolmogorov turbulence and the smaller generalized refractive-index structure parameter may lead to the higher average probability densities of signal vortex modes and lower average probability densities of crosstalk vortex modes. Lower-coherence radius or beam waist can give rise to less reduction of the normalized powers of the signal vortex modes, which is opposite to the normalized powers of crosstalk vortex modes.

OCIS codes: (010.1330) Atmospheric turbulence; (270.5290) Photon statistics; (270.5565) Quantum communications.
http://dx.doi.org/10.1364/PRJ.4.000030

1. INTRODUCTION

In recent years, the study of the stable vortex beams whose vortex model per photon can take an arbitrary value within a continuous range, either integer or noninteger, in units of $\hbar$ is a newly burgeoning field [1–5]. The propagation property of fractional vortice-imprinted Bessel beams in free space has been given attention both theoretically and experimentally [6–8]. It has been verified that vortices with fractional strength do not propagate unaffected in free space. However, neglecting their evolving intensity and vortex structure, a vortex integrated over the whole beam cross section is invariant under free-space propagation [7]. The fractional Bessel beams (nondiffracting vortex beams) are of special interest due to their properties of divergence-free propagation and self-repair, and have generated widespread interest in the last decade for applications in optical communications [9–13]. Götte proposed a quantum mechanical description of the beams with fractional topological charges [13], and a high-order Bessel nonvortex beam of fractional type (HOBNVBs-F) was introduced by Mitri [10–12]. Next, we developed the model of average probability densities and the normalized powers of the signal/crosstalk orbital angular momentum modes for the fractional-order Bessel–Gauss (FoBG) photon beams in the turbulent atmosphere of strong irradiance fluctuations [14]. On the other hand, we know that Kolmogorov's power spectral density model is widely used and accepted to describe wave propagation through atmospheric turbulence, but the experimental data in the last several decades shows that atmospheric turbulence generally possesses a structure different from the Kolmogorov model [8]. The Kolmogorov turbulence is actually an exception to non-Kolmogorov turbulence. When describing the effect of turbulence on fractional Bessel–Gauss photon beams in different conditions, it is better using non-Kolmogorov turbulence than Kolmogorov turbulence, which is especially embodied in its exponent value. As we know, there is almost no discussion with respect to the effects of non-Kolmogorov turbulence on the probability densities and the normalized powers of the vortex modes for FoBG photon beams in the weak and paraxial atmosphere channel.

In this paper, we analyze the influence of non-Kolmogorov turbulence on the vortex mode probability densities and the normalized powers for FoBG beams along the direction of the beam radius. Our aim is to exploit this changing process to present the effects of the weak non-Kolmogorov turbulence on Bessel–Gauss photon beams. We anticipate that this work will be particularly useful when applied to practical application for optical wireless communication. In Section 2, the models of the probability density for vortex modes and the normalized power of vortex per photon per unit length of a transverse slice of the beam for FoBG beams in non-Kolmogorov turbulence are established. The effects of fractional topological charges, turbulence strength (in weak fluctuation region), propagation distance, the non-Kolmogorov turbulence parameter, and wavelength on the probability densities of signal and crosstalk vortex modes of FoBG photon beams along the direction of the receiving plane are researched in Section 3. Conclusions are presented in Section 4.

2. MODE PROBABILITY DENSITY

In the weak fluctuation region [15] and in the half-space $z>0$, the normalized complex amplitude of FoBG beams in a cylindrical coordinate system (r,φ,z) can be expressed as [16]

$$\mathrm{FoBG}(r,\varphi,z)=\mathrm{FoBG}_{\mathrm{free}}(r,\varphi,z)\exp[\psi(r,\varphi,z)], \tag{1}$$

where $r=|\mathbf{r}|$, $\mathbf{r}=(x,y)$ is the two-dimensional position vector in the source plane; z is propagation distance; $\psi(r,\varphi,z)$ is the complex phase of waves propagating through turbulence; l_0 describes the topological charge of the helical structure of the wave front around a wave front singularity; and $\mathrm{FoBG}_{\mathrm{free}}(r,\varphi,z)$ is the normalized complex amplitude of the FoBG beam at the z plane in the free turbulence channel. In the paraxial region, the normalized complex amplitude $\mathrm{FoBG}_{\mathrm{free}}(r,\varphi,z)$ of a nondiffracting Bessel–Gauss photon beam with fractional topological charge has the form [7,15]

$$\begin{aligned}\mathrm{FoBG}_{\mathrm{free}}(r,\varphi,z)=&\frac{1}{\mu(z)}\frac{(\pm\mathrm{i})^{\gamma}\sin(\pm\pi\gamma)}{\pi}\\&\times\exp\left[-\mathrm{i}\frac{k_r^2 z}{2k\mu(z)}-\frac{r^2}{\mu(z)w_0^2}\right]\\&\times\sum_{l_0=-\infty}^{\infty}\frac{\mathrm{i}^{|l_0|}}{\pm\gamma-l_0}J_{|l_0|}\left[\frac{k_r r}{\mu(z)}\right]\exp(\mathrm{i}l_0\varphi),\end{aligned} \tag{2}$$

where $\mu(z)=1+\mathrm{i}z/z_R$, $z_R=kw_0^2/2$, $k=2\pi/\lambda$ is the wavenumber; w_0 is the beam waist at the $z=0$ plane; λ is the wavelength; z_R is the Rayleigh range; $J_{|l_0|}$ is the Bessel function of integer orders; $k_r=\xi k$ is the transverse wavenumber; and γ is the fractional index of any real number [7]. To keep it simple, we use C_γ to denote the term $\frac{(\pm\mathrm{i})^{\gamma}\sin(\pm\pi\gamma)}{\pi}\cdot\frac{\mathrm{i}^{|l_0|}}{\pm\gamma-l_0}$.

As we know, from the view of quantum theory, the atmospheric turbulence fluctuations disturb the complex amplitude of the propagating photon beam, which is no longer guaranteed to be in the original eigenstate of topological charge. The resulting photon beam now can be regarded as a superposition of the waves with new topological charge. Similar to the discussion of [7,17] for beams with integer topological charge, the FoBG is expanded as an integral with orthogonal basis $\exp(\mathrm{i}l\varphi)$ which carries topological charge l; then the complex amplitude $\mathrm{FoBG}(r,\varphi,z)$ of the FoBG beam can be written as

$$\mathrm{FoBG}(r,\varphi,z)=\sum_{|l_0|=-\infty}^{\infty}\beta_l(r,z)\exp(\mathrm{i}l\varphi), \tag{3}$$

where the term $\beta_l(r,z)$ is the mode amplitude of the vortex mode with topological charge l at the position (r,z) given by

$$\beta_l(r,z)=\frac{1}{2\pi}\int_0^{2\pi}\mathrm{FoBG}(r,\varphi,z)\exp(-\mathrm{i}l\varphi)\mathrm{d}\varphi. \tag{4}$$

As we all know, the mode probability density is equal to $|\beta_l(r,z)|^2$. In turbulent media, the mode probability density is associated with the ensemble average over turbulent medium, i.e., $\langle|\beta_l(r,z)|^2\rangle_{at}$, where $\langle\cdot\rangle$ denotes the average over the ensemble of the turbulent atmosphere. By Eqs. (1) and (4) and proceeding with the ensemble average of atmospheric turbulence for $\beta_l(r,z)\beta_l^*(r,z)$, where $*$ denotes complex conjugate, the ensemble averaging mode probability density $D_l(r,z)$ of vortex models l of an FoBG beam in paraxial channel ($k_r\to\infty$) is given by

$$\begin{aligned}D_l(r,z)=&\langle|\beta_l(r,z)|^2\rangle_{at}\\=&\left(\frac{1}{2\pi}\right)^2\int_0^{2\pi}\int_0^{2\pi}\mathrm{FoBG}_{\mathrm{free}}(r,\varphi,z)\\&\times\mathrm{FoBG}_{\mathrm{free}}^{*}(r',\varphi',z)\\&\times\langle\exp[\psi(r,\varphi,z)+\psi^{*}(r',\varphi',z)]\rangle_{at}\\&\times\exp[-\mathrm{i}l(\varphi-\varphi')]\mathrm{d}\varphi\mathrm{d}\varphi'.\end{aligned} \tag{5}$$

In the far-field region [15], $\langle\exp[\psi(r,\varphi,z)+\psi^{*}(r',\varphi',z)]\rangle_{at}$ is given by

$$\begin{aligned}&\langle\exp[\psi(r,\varphi,z)+\psi^{*}(r',\varphi',z)]\rangle_{at}\\&=\exp\left[-4\pi^2k^2z\int_0^1\mathrm{d}\xi\int_0^{\infty}\kappa\Phi_n(\kappa)(1-J_0(\kappa|\xi(\mathbf{r}-\mathbf{r}')|))\mathrm{d}\kappa\right],\end{aligned} \tag{6}$$

where $\Phi_n(\cdot)$ denotes the spatial power spectrum of atmospheric turbulence and $J_0(\cdot)$ is the Bessel function of the first kind with 0 order. For non-Kolmogorov turbulence, the spatial power spectrum is commonly given by the expression [18]

$$\Phi_n(\kappa)=A(\alpha)C_n^2\exp(-\kappa^2/\kappa_m^2)(\kappa^2+\kappa_0^2)^{-\alpha/2},\qquad 3<\alpha<4,$$

where α is the parameter of non-Kolmogorov turbulence, $\Gamma(\alpha)$ denotes the Gamma function, and $A(\alpha)=\Gamma(\alpha-1)\cos(\alpha\pi/2)/4\pi^2$; $\kappa_0=2\pi/L_{\mathrm{outer}}$ and $\kappa_m=\{2\pi\Gamma[(5-\alpha)/2]A(\alpha)/3\}^{1/(\alpha-5)}/L_{\mathrm{inner}}$, where L_{outer} and L_{inner} are the outer and inner scale of turbulence, respectively. C_n^2 is the generalized refractive-index structure parameter with units $m^{3-\alpha}$; for simplicity's sake, we set C_n^2 for FoGB beams as a constant to discuss the influence of α on the beam. To simplify the numerical discussion in Section 3, we set $L_{\mathrm{outer}}=\infty$ without considering the effect of outer scale, and $L_{\mathrm{inner}}=1$ mm [15].

In the paraxial approximation of the wave phase structure function, Eq. (6) can be expressed in the following form [15]:

$$\begin{aligned}\langle\exp[\psi(r,\varphi,z)+\psi^{*}(r',\varphi',z)]\rangle_{at}&\cong\exp\left[-\frac{|\mathbf{r}-\mathbf{r}'|^2}{\rho_0^2}\right]\\&=\exp\left[-\frac{r^2+r'^2-2rr'\cos(\varphi-\varphi')}{\rho_0^2}\right],\end{aligned} \tag{7}$$

where ρ_0 is the spatial coherence radius of a spherical wave propagating in the weak non-Kolmogorov turbulence [18,19] and given by

$$\rho_0=\left\{\frac{2\Gamma[(3-\alpha)/2](\alpha-1)}{\pi^{1/2}k^2\Gamma(1-\alpha/2)C_n^2 z}\right\}^{1/(\alpha-2)},\qquad 3<\alpha<4,$$

based on the integral expression [20]

$$\int_0^{2\pi}\exp[-\mathrm{i}n\varphi_1+\eta\cos(\varphi_1-\varphi_2)]\mathrm{d}\varphi_1=2\pi\exp(-\mathrm{i}n\varphi_2)I_n(\eta), \tag{8}$$

where $I_n(\eta)$ is the Bessel function of the second kind with n order. Making use of Eqs. (2), (5), and (7) as well as the Bessel function orthogonal completeness

$$\sum_{m=-\infty}^{\infty}\sum_{n=-\infty}^{\infty}J_m(x)J_n(x)=\begin{cases}\sum_{m=-\infty}^{\infty}|J_m(x)|^2, & m=n\\ 0, & m\neq n\end{cases},$$

we have the probability density of the vortex modes for FoBG beams in paraxial turbulence channel

$$D_l(r,z)=\frac{\sin^2(\pi\gamma)w_0^2}{\pi^2w^2(z)}\sum_{l_0=-\infty}^{\infty}\frac{1}{(\pm\gamma-l_0)^2}\left|J_{|l_0|}\left(\frac{k_r r}{\mu(z)}\right)\right|^2 \times\exp\left[-\left(\frac{1}{w^2(z)}+\frac{1}{\rho_0^2}\right)2r^2\right]I_{l-l_0}\left(\frac{2r^2}{\rho_0^2}\right), \quad (9)$$

where $w(z)=w_0\sqrt{1+z_R^2/z^2}$ is the Gaussian spot size and $\Delta l=l-l_0$ denotes the value of crosstalk. For $\Delta l=0$, $D_{l_0}(r,z)$ is the probability density of the signal vortex mode l_0 for FoBG beams, and for $\Delta l\neq 0$, $D_{l\neq l_0}(r,z)$ is the probability density of the crosstalk vortex mode $l=l_0+\Delta l$, which represents the probability density of the part of the energy launched into the signal vortex mode redistributed into other vortex modes by atmospheric turbulence [21]. The term C_γ^2 indicates the vortex model distribution for different fractional values γ when l_0 changes (see Fig. 1).

The normalized power of vortex per photon per unit length of a transverse slice of the beam is calculated with the expression [7]

$$L_z(l)=\hbar\sum_{l=-\infty}^{\infty}\frac{lBP_l}{\sum_{l=-\infty}^{\infty}BP_l}, \quad (10)$$

where B is the is the beam width of the channel, $\sum_{l=-\infty}^{\infty}BP_l$ is the beam power, and BP_l is the power of each vortex mode with topological charge l with and given by [7]

$$P_l=\int_0^{\infty}D_l(r,z)r\mathrm{d}r =\frac{\sin^2(\pi\gamma)w_0^2}{\pi^2w^2(z)}\sum_{l_0=-\infty}^{\infty}\frac{1}{(\pm\gamma-l_0)^2}\times\int_0^{\infty}\left|J_{|l_0|}\left(\frac{k_r r}{\mu(z)}\right)\right|^2 \times\exp\left[-\left(\frac{1}{w^2(z)}-\frac{1}{\rho_0^2}\right)2r^2\right]\times I_{l-l_0}\left(\frac{2r^2}{\rho_0^2}\right)r\mathrm{d}r. \quad (11)$$

Similarly, for $l=l_0$, $L_z(l_0)$ expresses the normalized power of the signal vortex mode for FoBG photon beams and, for $l\neq l_0$, $L_z(l)$ is the normalized power of the crosstalk vortex modes.

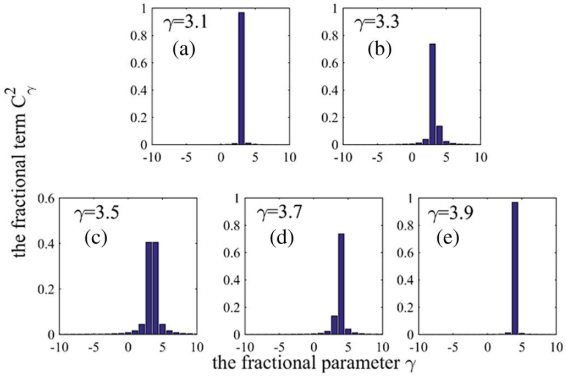

Fig. 1. Distribution of vortex models with fractional topological charge γ when l_0 changes. Every subplot has a peak at the nearest integer to γ. When $\gamma=3.5$ (half-integer), this results in two peaks of equal height at the two neighboring integers. The spread in the distribution is determined by the fractional value γ.

3. NUMERICAL DISCUSSION

As we all know, the longer wavelength λ is beneficial to the propagation of photon beams for less attenuation and lower crosstalk. Besides, it is entirely reasonable that the average probability density of signal vortex modes and signal normalized powers decrease, and the average crosstalk probability of vortex modes and crosstalk normalized powers increase when the propagation distance z increases. Then, we do not discuss the influences owed to the wavelength λ and the propagation distance z. To simplify, in the following figures, we now define mode probability as average probability density ($D_{l_0}(r,z)$) of the signal vortex modes, and crosstalk probability as the average probability density ($D_{l\neq l_0}(r,z)$) of the crosstalk vortex modes.

First, we study the effects of the fractional order of topological charge l, the fractional parameter γ, the non-Kolmogorov turbulence coherence radius ρ_0 (in weak fluctuation region), and beam waist w_0 on the average probability densities $D_l(r,z)$ along the direction of r for FoBG beams. The simulation results are shown in Figs. 2–5. In Fig. 2, we evaluate performance of average probability densities $D_l(r,z)$ along the direction of the beam radius r for FoBG beam with $w_0=0.1m$, $\xi=0.01$, and $\Delta l=0$, 1, 2, 3, and 4. The parameters for the simulation of atmospheric turbulence channel are as follows: $z=1km$, $\alpha=11/3$, and $C_n^2=10^{-15}m^{3-\alpha}$. From Fig. 2, we can see that crosstalk probability $D_{l\neq l_0}(r,z)$ decreases with the increase of topological charge deviation Δl and it drops rapidly after the slow growth with the increase of r. When r is large enough (in Fig. 2, $r>0.2m$), mode probability $D_{l_0}(r,z)$ and crosstalk probability $D_{l\neq l_0}(r,z)$ tend to be the same. The results show that we can obtain the higher signal crosstalk probability ratio only in the circle region of radius $r<0.2m$, and the center of the circle region is the beam center. So in the next context, we adopt the circle region of radius $r<0.2m$.

In Fig. 3, the average probability density $D_l(r,z)$ is plotted as a function of the beam radius r for topological charge deviation $\Delta l=0$ and 1, with $w_0=0.10m$, $\xi=0.01$, $z=1km$, $\alpha=11/3$, and $C_n^2=10^{-15}m^{3-\alpha}$. Figures 3(a) and 3(b) are for $\gamma=3.1$, 3.3, 3.5, 3.7, and 3.9, respectively. As is seen from Fig. 3, the $D_l(r,z)$ for $\gamma=3.1$, 3.3, 3.7, and 3.9 are the vibration curves which are around the curve of $\gamma=3.5$. Figure 3(a) indicates that mode probability decreases with the increase of r, while the crosstalk probability decays after the increase in the area close to the circle area in Fig. 3(b). Figures 3(a) and 3(b) show that the curve is without

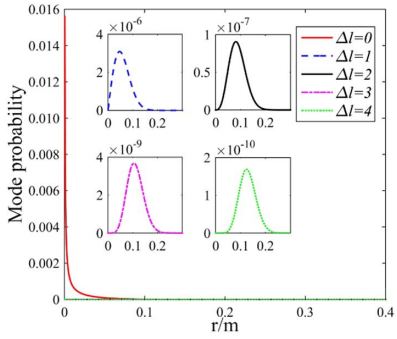

Fig. 2. Average mode probability $D_l(r,z)$ of FoBG beam along the direction of the beam radius r for different values of Δl.

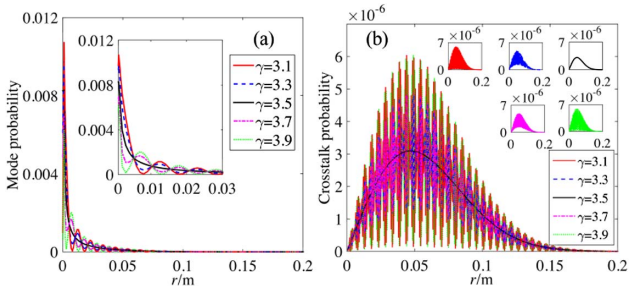

Fig. 3. Average probability densities $D_l(r,z)$ of vortex modes for fractional FoBG beam along the direction of the beam radius r with different values of γ. (a) $\Delta l = 0$, mode probability; (b) $\Delta l = 1$, crosstalk probability.

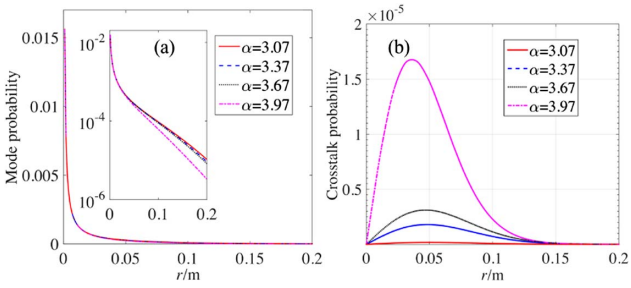

Fig. 4. Average probability densities $D_l(r,z)$ of vortex modes for fractional FoBG beam along the direction of the beam radius r with different values of α. (a) $\Delta l = 0$, mode probability; (b) $\Delta l = 1$, crosstalk probability.

vibration when the value of γ is half-integer. And the more close the value of γ is to half-integer, the closer its curve tends to the curve with $\gamma = 3.5$. In order to facilitate the beam properties, we set $\gamma = 3.5$.

Figures 4 and 5 present how the various parameters of atmospheric turbulence affect the average probability densities $D_l(r,z)$. Figure 4(a) is a plot of the average mode probability $D_{l_0}(r,z)$ versus the varied beam radius r for the different non-Kolmogorov turbulence parameters α. The curve associated with $\alpha = 3.67$ corresponds to Kolmogorov turbulence. The curves in Fig. 4(a) are consistent with [18] in that the smaller α comes with the larger $D_{l_0}(r,z)$ in the receiving plane for any given propagation distance; the reason is that the spatial coherence radius ρ_0 tends to infinity when α approaches 3. That is, the interruption of the turbulence on the photon beams is very weak, and a high $D_{l_0}(r,z)$ is acquired. However, when α is close to 4, the wave aberration caused by turbulence is a pure wavefront tilt, which shifts the beam off-axis and results in the beam center being away from the receiving plane [18]. Thus, $D_{l_0}(r,z)$ decreases as α approaches 4. The relationship between the average crosstalk probability $D_{l\neq l_0}(r,z)$ and the α of non-Kolmogorov turbulence is revealed by Fig. 4(b). When the propagation distance z is given, the $D_{l\neq l_0}(r,z)$ of FoBG photon beams increases rapidly when α changes from 3.07 to 3.97 near the beam center regions (about $r < 0.04m$). When detection position is far away from the beam center in the receiving plane, all the curves in Fig. 4(b) tend to be same.

Figure 5 is constructed to assess how the non-Kolmogorov turbulence coherence radius C_n^2 affects the average probability densities $D_l(r,z)$ with varied beam radius r. The curves in Fig. 5(a) show that increasing r makes mode probability $D_{l_0}(r,z)$ decrease sooner, while increasing C_n^2 doesn't make the signal probability density change apparent. It is important to note that crosstalk probability $D_{l\neq l_0}(r,z)$ increases with the lower C_n^2 near the beam center (about $r < 0.04m$), and the main energy still remains at the transmit signal channel. However, crosstalk probability decays and the energy of the adjacent channel decreases immediately as the detection position moves away from the beam center. For instance, all the curves slowly tend to overlap; namely, the effects of different C_n^2 value on crosstalk probability densities become less distinct when $r > 0.15m$.

Figure 6 investigates the average probability $D_l(r,z)$ as a function of beam radius r for a FoBG beam with topological charge deviation $\Delta l = 0$ and 1, $\gamma = 3.5$, and $\xi = 0.01$ for $w_0 = 0.02m$, 0.05 m, 0.08 m, and 0.10 m, respectively. The parameters of the atmospheric turbulence channel for the simulation are as follows: $z = 1km$, $\alpha = 11/3$, and $C_n^2 = 10^{-15}m^{3-\alpha}$. Figure 6(a) shows that increasing w_0 makes mode probability decay slowly. The results of Fig. 6(b) reveal that higher w_0 corresponds to the higher crosstalk probability densities and makes the curve peak away from the beam center.

For the sake of simplicity, we will discuss the impact of ρ_0 on the mode probability densities and normalized powers instead of the basic parameters α and C_n^2. The normalized powers $L_z(l)$ of signal and crosstalk vortex modes for the parameters $\alpha = 11/3$, $C_n^2 = 10^{-15}m^{3-\alpha}$, $w_0 = 0.10m$, and $\Delta l = 0$, 1, 2, 3, and 4 are shown in Fig. 7. Here we see that the crosstalk-normalized powers $L_z(l \neq l_0)$ between vortex modes decrease with the increasing of Δl.

Finally, the effects of ρ_0 and w_0 on the normalized powers $L_z(l)$ of signal or crosstalk vortex modes per photon per unit length of a transverse slice for FoBG beams are shown in Fig. 8. To do that, we fix the parameters $\gamma = 3.5$ and

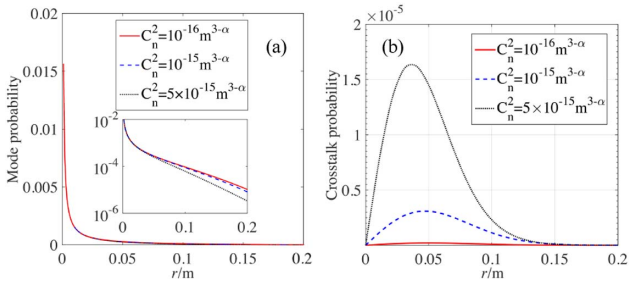

Fig. 5. Average probability densities $D_l(r,z)$ of vortex modes for fractional FoBG beam along the direction of the beam radius r with different values of C_n^2. (a) $\Delta l = 0$, mode probability; (b) $\Delta l = 1$, crosstalk probability.

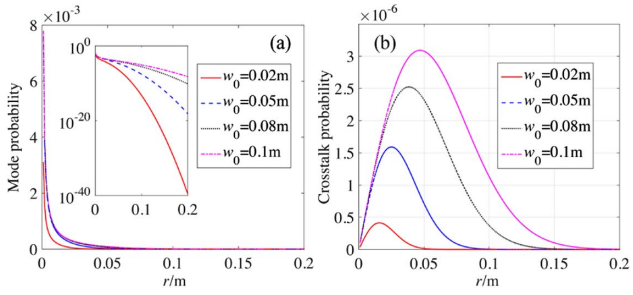

Fig. 6. Average probability densities $D_l(r,z)$ of vortex modes for fractional FoBG beam along the direction of the beam radius r with different values of beam waist w_0. (a) $\Delta l = 0$, mode probability; (b) $\Delta l = 1$, crosstalk probability.

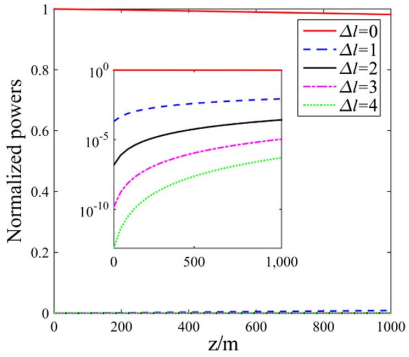

Fig. 7. Normalized powers $L_z(l)$ of fractional vortex modes for FoBG beam along the direction of the transmission distance z with different values of Δl.

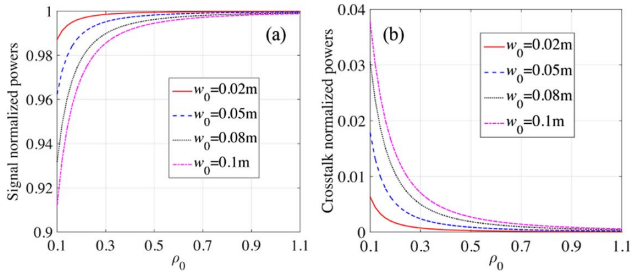

Fig. 8. Normalized powers $L_z(l)$ of fractional vortex modes for FoBG beam along coherence radius r with different values of beam waist w_0. (a) $\Delta l = 0$, signal normalized powers; (b) $\Delta l = 1$, crosstalk normalized powers.

$\xi = 0.01$. Lower ρ_0 can give rise to increase of the normalized power of the signal vortex mode $L_z(l_0)$ and decrease of the normalized powers of the crosstalk vortex modes $L_z(l \neq l_0)$. Obviously, greater w_0 can enhance the normalized power of the signal vortex mode and reduce the normalized powers of crosstalk vortex modes.

4. CONCLUSION

In conclusion, the model of probability densities and the normalized powers of signal or crosstalk vortex modes for FoBG photon beams in weak fluctuation turbulent atmosphere have been developed. Our results show that average mode probability $D_{l_0}(r,z)$ and average crosstalk probability $D_{l\neq l_0}(r,z)$ are the same when beam radius r is large enough. For fractional order Bessel–Gauss beams, when r varies, $D_l(r,z)$ oscillates except γ is half-integer. For the half-integer beams, the increases of α and C_n^2 result in the degradation of $D_{l_0}(r,z)$, and average crosstalk probability $D_{l\neq l_0}(r,z)$ drops rapidly after the slow growth as r increases, namely average crosstalk probability curves have peaks. Near the central region of the beam, enlarging Δl or minimizing α, C_n^2, and w_0 can make the $D_{l\neq l_0}(r,z)$ decrease. Furthermore, lower ρ_0 and w_0 can give rise to less reduction of the turbulence effect on the normalized power of signal vortex mode. Compared with signal normalized powers, the opposite changes in tendency of crosstalk-normalized powers are observed.

ACKNOWLEDGMENT

This work is supported by the Natural Science Foundation of Jiangsu Province of China (Grant No. BK20140128), the National Natural Science Foundation of Special Theoretical Physics (Grant No. 11447174), and the Fundamental Research Funds for the Central Universities (JUSRP51517).

REFERENCES

1. J. Leach, E. Yao, and M. J. Padgett, "Observation of the vortex structure of a non-integer vortex beam," New J. Phys. **6**, 71 (2004).
2. W. N. Plick, M. Krenn, R. Fickler, and S. Ramelow, "Quantum orbital angular momentum of elliptically symmetric light," Phys. Rev. A **87**, 033806 (2013).
3. M. V. Berry, "Optical vortices evolving from helicoidal integer and fractional phase steps," J. Opt. A **6**, 259–268 (2004).
4. J. C. Gutiérrez-Vega, "Fractionalization of optical beams: II. Elegant Laguerre-Gaussian modes," Opt. Express **15**, 6300–6313 (2007).
5. J. B. Götte, K. O'Holleran, D. Preece, F. Flossmann, S. Franke-Arnold, and S. M. Barnett, "Light beams with fractional orbital angular momentum and their vortex structure," Opt. Express **16**, 993–1006 (2008).
6. S. H. Tao and X. Yuan, "Self-reconstruction property of fractional Bessel beams," J. Opt. Soc. Am. A **21**, 1192–1197 (2004).
7. J. C. Gutiérrez-Vega and C. López-Mariscal, "Nondiffracting vortex beams with continuous orbital angular momentum order dependence," J. Opt. A **10**, 015009 (2008).
8. E. Golbraikh, H. Branover, N. S. Kopeika, and A. Zilberman, "Non-Kolmogorov atmospheric turbulence and optical signal propagation," Nonlinear Processes Geophys. **13**, 297–301 (2006).
9. J. C. Gutirrez-Vega and C. Lopez-Mariscal, "Nondiffracting vortex beams with continuous orbital angular momentum order dependence," J. Opt. A **10**, 015009 (2008).
10. F. G. Mitri, "Vector wave analysis of an electromagnetic high-order Bessel vortex beam of fractional type," Opt. Lett. **36**, 606–608 (2011).
11. F. G. Mitri, "High-order Bessel nonvortex beam of fractional type," Phys. Rev. A **85**, 025801 (2012).
12. F. G. Mitri, "High-order Bessel non-vortex beam of fractional type: II. Vector wave analysis for standing and quasi-standing laser wave tweezers," Eur. Phys. J. D **67**, 135 (2013).
13. J. B. Götte, S. Franke-Arnold, R. Zambrini, and S. M. Barnett, "Quantum formulation of fractional orbital angular momentum," J. Mod. Opt. **54**, 1723–1738 (2007).
14. J. Gao, Y. Zhang, W. Dan, and Z. Hu, "Turbulent effects of strong irradiance fluctuations on the orbital angular momentum mode of fractional Bessel Gauss beams," Opt. Express **23**, 17024–17034 (2015).
15. L. C. Andrews and R. L. Phillips, *Laser Beam Propagation Through Random Media*, 2th ed. (SPIE, 2005).
16. C. López-Mariscal, D. Burnham, D. Rudd, and D. McGloin, "Phase dynamics of continuous topological upconversion in vortex beams," Opt. Express **16**, 11411–11422 (2008).
17. Y. Jiang, S. Wang, J. Zhang, and J. Ou, "Spiral spectrum of Laguerre-Gaussian beams propagation in non-Kolmogorov turbulence," Opt. Commun. **303**, 38–41 (2013).
18. C. Rao, W. Jiang, and N. Ling, "Spatial and temporal characterization of phase fluctuations in non-Kolmogorov atmospheric turbulence," J. Mod. Opt. **47**, 1111–1126 (2000).
19. X. Sheng, Y. Zhang, X. Wang, Z. Wang, and Y. Zhu, "The effects of non-Kolmogorov turbulence on the orbital angular momentum of photon-beam propagation in a slant channel," Opt. Quantum Electron. **43**, 121–127 (2012).
20. I. S. Gradshteyn and I. M. Ryzhik, *Table of Integrals, Series and Products*, 6th ed. (Academic, 2000).
21. J. A. Anguita, M. A. Neifeld, and B. V. Vasic, "Turbulence-induced channel crosstalk in an orbital angular momentum-multiplexed free-space optical link," Appl. Opt. **47**, 2414–2429 (2008).